Volume 16 Number 14 1988 Nucleic Acids Research

Sequence-directed bends of DNA helix axis at the upstream activation sites of α-cell-specific genes in yeast

Kaoru Inokuchi*, Akiko Nakayama and Fumio Hishinuma

Laboratory of Molecular Genetics, Mitsubishi Kasei Institute of Life Sciences, 11 Minamiooya, Machida, Tokyo 194, Japan

Received May 24, 1988; Accepted June 20, 1988

ABSTRACT

The MFα1 gene of Saccharomyces cerevisiae, a major structural gene for mating pheromone α factor, is an α-cell-specific gene whose expression is regulated by the mating-type locus, MAT. Two upstream activation sites ($UAS_{MF\alpha1}$s), which are binding sites for an activator protein, MATα1, mediate α-cell-specific expression of this gene. We show here that DNA fragments containing the $UAS_{MF\alpha1}$ region exhibited anomalous slow electrophoretic mobilities on gels at lower temperature, but not at higher temperature, that is characteristic of bent DNA. We confirmed the sequence-directed bend at the $UAS_{MF\alpha1}$ region by employing a circular permutation analysis and a DNA cyclization assay. Deletion analyses revealed the existence of two bends in this region, each of which overlaps each $UAS_{MF\alpha1}$ element. The two bends were almost in phase; they lie in a nearly same plane with a same direction. We also show the existence of sequence-directed bend at the UAS region of the STE3 gene, another α-specific gene in S. cerevisiae. These bent DNAs may be involved in transcriptional regulation of this set of genes.

INTRODUCTION

Most promoters recognized by RNA polymerase II in yeast consist of two elements (for reviews see references 1, 2). The first element, the highly conserved TATA box, is usually located within 100 base pairs (bp) upstream of the transcription start point(s). This element, along with sequences at the start of transcription initiation, contains all the information necessary to specify the transcription start point(s). A second class of elements, termed upstream activation sites (UASs), determines the efficiency of transcription in response to particular physiological signals . Such a signal is thought to be transmitted to the UAS of a target gene by the mediation of a regulatory protein(s). Genes subject to a common control mechanism contain UASs that are similar in DNA sequence. UASs resemble mammalian enhancer elements in that they can activate

transcription irrespective of their orientation and of their distance from TATA box (3, 4). Recently, it has been shown that the yeast UAS_G can act as an activation element in mammalian cells in the presence of the yeast trans-activator protein, GAL4 (5, 6). Therefore, the molecular mechanisms involved in transcription activation should be very similar in yeast and mammal.

The yeast Saccharomyces cerevisiae possesses a set of α-specific genes, such as MFα1, MFα2 and STE3, which is expressed only in haploid α cells, not in **a** or diploid **a**/α cells. Expression of this set of genes is regulated by MAT, the mating type locus (7). The 5'-flanking region (about 950 bp) of the MFα1 gene, a major structural gene for mating pheromone α factor, is sufficient to confer α-specific expression of the gene (8, 9). We have previously identified a TATA box and two closely related, tandemly arranged upstream activation sites ($UAS_{MF\alpha1}$) as necessary elements for maximum level of MFα1 transcription (9)(Figure 1a). Synthetic versions of homologous 28 bp sequences present in the $UAS_{MF\alpha1}$ region, one at position -367 to -340 ($UAS_{MF\alpha1}$-1) and the other at -314 to -287 ($UAS_{MF\alpha1}$-2), can activate UAS-less CYC1 gene and bring it under α-cell-specific expression (Inokuchi and Nakayama, in preparation)(We have numbered the first letter of the initiation codon +1 throughout this work except for Figure 2). $UAS_{MF\alpha1}$s are the binding sites for activator proteins, the MATα1 gene product and PRTF (10; Inokuchi, unpublished data). The MATα1 gene is expressed only in α cells and the product is required for expression of α-specific gene (7-9, 11, 12), thus $UAS_{MF\alpha1}$s can confer cell type-specific expression of the MFα1 gene. As expected, $UAS_{MF\alpha1}$s act in both orientations and at variable distances with respect to the mRNA start points. The most intriguing feature of these $UAS_{MF\alpha1}$ elements is that they act in a synergistic fashion; lack of either element caused reduced expression levels that are 6- to 45-fold less than that of intact promoter in α cells (9).

Recent works have revealed the existence of sequence-directed bend (static bend) of DNA helix axis. The first naturally occurring bent DNA was proposed for the kinetoplast DNA isolated from the trypanosome mitochondria (13). Hydrodynamic, electrophoretic, electronmicroscopic and hydroxyl-radical-footprinting experiments have confirmed the bent helical structure of the kinetoplast DNA (13-18). Subsequently, sequence-directed bends have been discovered in other

DNA molecules that are important for biological function: the replication origins of bacteriophage λ (19, 20), simian virus 40 (21, 22), plasmid pT181 (23); a yeast autonomously replicating sequence, a putative replication origin (24); the hisR promoter in Salmonella typhimurium (25) and the ompF promoter in Escherichia coli (26). Almost all of these bent regions contain periodically spaced runs of (dA•dT)s with one run per helical repeat, leading to the suggestion that (dA•dT) tract deforms the DNA helix axis by some mechanism (27). Although the sequence-directed bent helical structures seem to be important for the regulation of gene expression and DNA replication, a role of bends in such processes remains to be studied.

Here, we provide evidence that the $UAS_{MF\alpha1}$ region contains two sequence-directed bends, each of which overlaps each $UAS_{MF\alpha1}$ element. The relative directions of these bends are almost the same. Furthermore, we show the existence of a sequence-directed bend at the UAS region of the STE3 gene, another α-specific gene in yeast.

MATERIALS AND METHODS

Enzymes and chemicals

Restriction endonucleases, nuclease S1, exonuclease III, DNA polymerase I large fragment (Klenow), T4 polynucleotide kinase, and T4 DNA ligase were purchased from Toyobo and New England Biolabs. BamHI linkers (8-mer, 5'-dCGGATCCG; 10-mer, 5'-dCCGGATCCGG; 12-mer, 5'-dCCCGGATCCGGG), BglII linkers (8-mer, 5'-dCAGATCTG; 10-mer, 5'-dGCAGATCTGC) and dideoxy sequencing kit were obtained from Takara Shuzo. [γ-^{32}P]ATP and [α-^{32}P]dCTP were from Amersham. Phage λ DNA and φX174 DNA were from Toyobo.

DNA manipulation

Escherichia coli strain YO160recA was employed as the host to propagate plasmids. Yeast transformation was performed by the lithium ion method (28). Other procedures used were described previously (29).

Plasmid constructions

pAKI044. To construct tandem dimers of the 513 bp PstI (-739)/NsiI (-226) fragment, plasmid pINK002 (9) was digested with PstI and NsiI. The 513 bp fragment was isolated through agarose gel electrophoresis and inserted into the NsiI site of pINK002 to generate pAKI044.

Insertion mutant plasmids. We inserted various sets of BglII (8- and

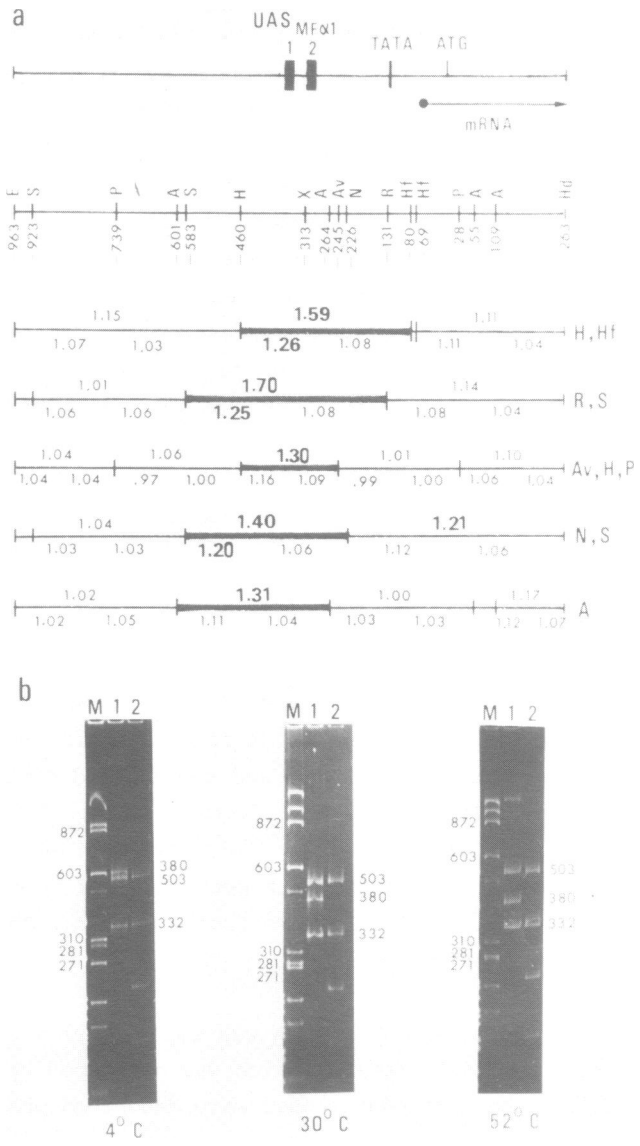

Fig. 1. Electrophoretic analysis of DNA fragments carrying the MFα1 region. (a) Features of MFα1. The boxes represent the two $UAS_{MF\alpha1}$ elements. The functional TATA box is located at position -128 to -122 and the mRNA start points are at -59, -56 and -53 (9). The 1226 bp of EcoRI/HindIII fragment was digested with the various restriction enzymes indicated, and the R values measured as described in Materials and methods. Electrophoresis was carried out at 4°C, 30°C or 52°C. Correct assignment of the DNA bands was determined by digestion with a second enzyme. The R values are indicated over (4°C) and under (left,

30°C; right, 52°C) the lines. Fragments where R>1.2 are indicated in bold type. Fragments where $R_{40°C}$>1.3 are indicated by thick lines. E, EcoRI; S, Sau3A; P, PstI; A, AluI; H, HhaI; X, XmnI; Av, AvaII; N, NsiI; R, RsaI; Hf, HinfI; Hd, HindIII. (b) Mobilities of DNA fragments in 7.5% polyacrylamide gel. The 1226 bp of EcoRI/HindIII fragment was digested with HhaI and HinfI (lane 1) or with HhaI, HinfI and XmnI (lane 2). Actual length (bp) of each fragment is indicated on the right. Lane M displays φX174 DNA cut with HaeIII. Some of the sizes of the marker fragments are given on the left.

10-mer) and BamHI (8-, 10- and 12-mer) linkers into the XmnI site (position -313; between the two $UAS_{MF\alpha1}$ elements, Figure 5) of plasmid pAKI039-30 (9) to generate insertion mutant plasmids. All the DNA sequences of insertion mutants were verified directly by the dideoxy DNA sequencing method (30) using a synthetic primer.

DNA bend assay

DNA was digested with restriction enzymes indicated, ethanol-precipitated and the electrophoretic mobilities of the fragments measured in 7.5% polyacrylamide gels (7.26% acrylamide, 0.24% N, N'-methylene-bis-acrylamide). The gel was run in 50 mM Tris-borate (pH 8.3) and 1 mM EDTA (TBE buffer), with the gel composed of the same buffer. Electrophoresis were at 7.6Vcm^{-1} at 4°C, 4.4Vcm^{-1} at 30°C and 2.4Vcm^{-1} at 52°C. To visualize DNA, gels were stained with ethidium bromide (0.5 μg/ml) for 20 to 30 min. Size markers used are φX174 HaeIII, φX174 AluI, pBR322 HapII, pBR322 AluI, λ PstI, and λ SspI. Some of these marker fragments migrated more slowly than expected. For example, the 281 bp fragment of φX174 shows retarded migration at 4°C (24)(Figure 1b). Therefore, we selected those fragments as size markers which migrated "normally", that is, those showing almost identical migration at either of these temperatures.

DNA cyclization assay

Fragment 2-Bam and fragment 6-Bam were 5'-end labeled with T4 polynucleotide kinase and [γ-^{32}P]ATP. Ligation reactions were carried out at 20°C in 600 μl of ligation buffer (66 mM Tris-HCl(pH 7.6), 10 mM $MgCl_2$, 10 mM dithiothreitol, and 1 mM ATP) containing 10 ng of 5'-end-labeled fragment 2-Bam or fragment 6-Bam. T4 DNA ligase (0.2 units) was added at time 0. At given times, 100 μl aliquotes were removed and immediately quenched in phenol-chloroform. The aqueous phase was extracted with ether and precipitated with ethanol. The products were run on a 4% polyacrylamide gel in TBE buffer, then the gel was dried and exposed against X-lay film.

RESULTS

Anomalous electrophoretic behavior of DNA fragments carrying the $UAS_{MF\alpha1}$ elements

Figure 1 shows electrophoretic behavior of DNA restriction fragments of the *MFα1* gene. The mobilities were compared to DNA fragments derived from φX174, pBR322 and λ DNAs (see Materials and methods). We observed that restriction fragments carrying the $UAS_{MF\alpha1}$ region migrated with an abnormally low mobility under nondenaturing electrophoretic conditions at 4°C and at 30°C. For example, a 380 bp *HhaI*/*HinfI* fragment, which contains both the $UAS_{MF\alpha1}$ elements, migrated to a position of a 603 bp fragment at 4°C, being more slowly than a 503 bp fragment (Figure 1b, left). Correct assignment of the 380 bp fragment was determined by digestion with a second enzyme, *XmnI*, which cut only this fragment (compare lane 1 with lane 2). This anomalous electrophoretic behavior persisted at the physiological temperature of 30°C, although a degree of anomaly was less prominent than that at 4°C (Figure 1b, middle). In contrast, mobility was close to normal when the gel was run at 52°C (Figure 1b, right).

Several restriction fragments spanning the $UAS_{MF\alpha1}$ region were tested for abnormal electrophoretic behavior and their R values were determined (R=ratio of the apparent number of base pairs to the actual number of base pairs)(Figure 1a). All DNA fragments containing the 196 bp region between the *HhaI* (-460) and *AluI* (-264) sites had R values over 1.30 at 4°C (R_{4^oC}). This 196 bp region contains both the $UAS_{MF\alpha1}$ elements (-367 to -340 and -314 to -287). The R values at 30°C (R_{30^oC}) of these DNA fragments were found to be over 1.11, whereas the values at 52°C (R_{52^oC}) were below 1.09. These results indicate that the retarded migration cannot be due to simple denaturation of DNA fragments, because temperature would have the opposite effect on migration.

These features, anomalous slow electrophoretic mobility at lower temperature and close to normal mobility at higher temperature, are characteristic of the bent DNA molecules observed in kinetoplast DNA (13-16), replication origins of λ phage, SV40, plasmid pT181 and yeast (20-24), *hisR* promoter of *S. typhimurium* (25) and *ompF* promoter of *E. coli* (26). Several lines of evidence indicate that the $UAS_{MF\alpha1}$ region indeed contains bent DNA structure (see below).

Bend center is located between the two $UAS_{MF\alpha1}$ elements

A property of bent DNA is the retarded electrophoretic mobility which is more pronounced when the bend is near the center of the fragment (14, 15). To test the $UAS_{MF\alpha1}$ region for this property, we used the circular permutation analysis (15)(Figure 2). We constructed tandem dimers of the 513 bp PstI (-739)/ NsiI (-226) fragment carrying the two $UAS_{MF\alpha1}$ elements (pAKI044, see Materials and methods). Cleavage of DNA with restriction enzymes PstI and NsiI yields the complementary protruding ends each other and the end can be ligated, however, the resultant junction site cannot be cleaved with either of the enzymes. The 1026 bp PstI/NsiI fragment shown in Figure 2a was isolated from pAKI044 by digestion with PstI and NsiI, and cleaved with a variety of enzymes which cut once within the 513 bp sequence. Digestion with these enzymes yields molecules of identical size (513 bp) and nucleotide composition with variation in the position of $UAS_{MF\alpha1}$s relative to the molecular ends.

Figure 2b shows the electrophoretic mobilities at 4°C of these molecules. The result shows that significantly lower mobility was observed as the two $UAS_{MF\alpha1}$ elements were moved nearer the center of the molecule. In contrast, the mobility was almost normal when $UAS_{MF\alpha1}$ loci were close to the end of the fragment. As plotted in Figure 2c, the relative mobility of the fragment will reach a maximum at a position between the two $UAS_{MF\alpha1}$ elements, when the gels were run at 4°C or at 30°C. All the fragments were found to migrate almost normally when run at 52°C. These results are consistent with the DNA bending model, which predicts that the extent of mobility anomaly is dependent upon the position of the bend with respect to the fragment ends and that the maximal retardation is found when the bend is at the center of the fragment (14, 15). These results further indicate that the bend center is located between the two $UAS_{MF\alpha1}$ elements.

DNA cyclization assay confirms the sequence-directed bend

We confirmed the sequence-directed bend at the $UAS_{MF\alpha1}$ region by employing a DNA cyclization assay (20, 31, 32). For a given length of DNA, existence of a bend will increase the probability that the two ends of a linear DNA molecule are in close proximity. This effect will be more pronounced in the case of the sequence-directed bend being located at the center of the molecule, rather than located close to the ends. These differences can easily be detected by assaying the intramolecular ligation rates.

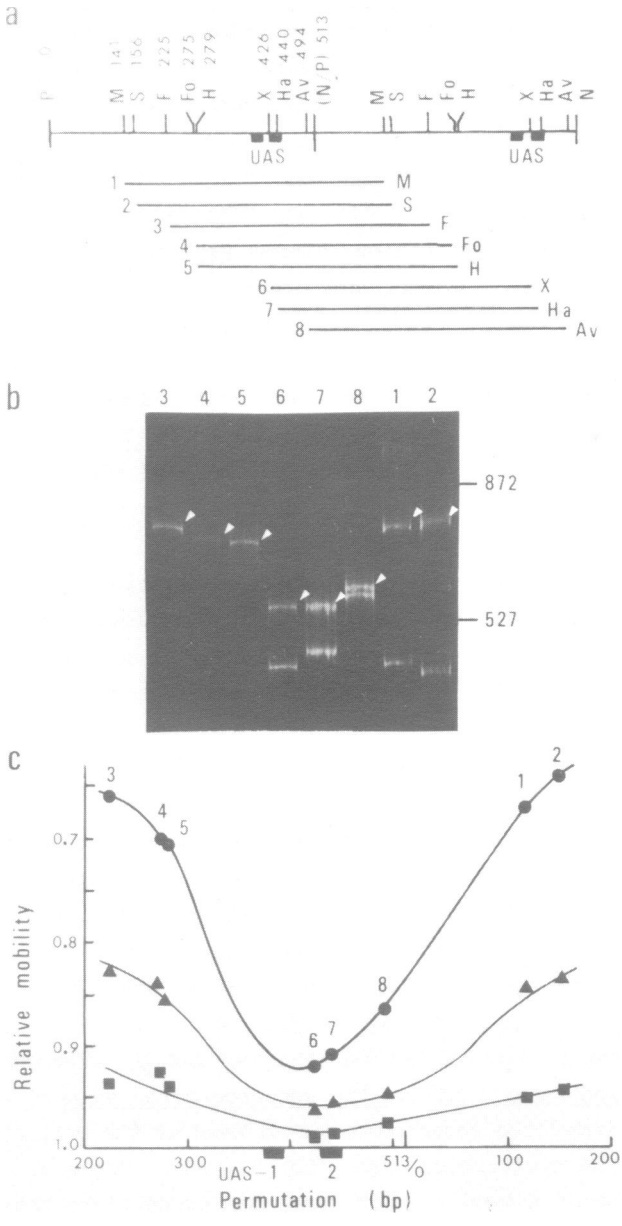

Fig. 2. Circular permutation analysis of the 513 bp fragment containing $UAS_{MF\alpha1}$s. (a) Restriction map of the 513 bp PstI/NsiI fragment as a tandem dimer. The restriction sites which occur once in each unit of the dimer are indicated and their positions within the fragment are noted above the site. The PstI and NsiI sites are at

positions -739 and -226 with respect to the first letter of initiation codon, respectively. Dark boxes represent the $UAS_{MF\alpha1}$ elements. Each permuted fragment is shown as a line under the map bounded by its recognition sites and the fragment is numbered on the left and named by the enzyme used to generate it on the right. M, MnlI; F, Fnu4HI; Fo, FokI; Ha, HaeIII. Other abbreviations used are as in Figure 1. (b) Electrophoresis of the permutated fragments in a 7.5% polyacrylamide gel at 4°C. The 1026 bp PstI/NsiI tandem dimer fragment was digested with MnlI, Sau3A, Fnu4HI, FokI, HhaI, XmnI, HaeIII or AvaII. Lanes are indicated according to the numbers in panel a. White arrowheads indicate the permuted fragments derived from each restriction digest. Positions of the 872 bp and 527 bp fragments derived from HaeIII cut ϕX174 and HapII cut pBR322 DNA, respectively, are indicated on the right. (c) Mapping of the bend center. The relative mobilities of the permuted fragments are plotted against the positions of the restriction site (permutation) in one unit of the tandem dimer. Relative mobility is represented as observed distance migrated per expected migration distance. The positions of two $UAS_{MF\alpha1}$ elements are indicated by dark boxes. ●, 4°C; ▲, 30°C; ■, 52°C.

We generated two linear DNA species having identical length, nucleotide compositions and sticky ends but differing in the location of the two $UAS_{MF\alpha1}$ elements with respect to the ends. The 513 bp Sau3A fragment (fragment 2, Figure 2a) was end-filling and an 8 bp long BamHI linker was ligated to each end of the molecule (fragment 2-Bam). The same linker was also ligated to each end of the XmnI fragment (fragment 6, Figure 2a) to generate fragment 6-Bam. The linear DNAs were 5'-end labeled and the products of ligation reaction (carried out at 20°C) were loaded onto polyacrylamide gels (Figure 3). The DNA concentration in the reaction mixture was set beneath 20 ng/ml to minimize oligomer formation. The lower band corresponding to the starting linear fragment (Figure 3a, L) disappeared after exonuclease III digestion, while the product shown by C persisted (data not shown). This assign the upper band to the circular molecule. The cyclization rate of fragment 2-Bam was about 10 times that of fragment 6-Bam (Figure 3b). Since fragment 2-Bam has the two $UAS_{MF\alpha1}$ elements at the center of the molecule in contrast to fragment 6-Bam having these elements near the ends, this result confirms the sequence-directed bend of DNA helix axis at the $UAS_{MF\alpha1}$ region.

$UAS_{MF\alpha1}$ region contains two sequence-directed bends

To localize the bent DNA region more precisely, we used two sets of MFα1 promoter deletions constructed previously (9). The first series of deletions, upstream deletions, were designated ΔX, where X indicates the nucleotide number of the deletion end (Figure 4, upper

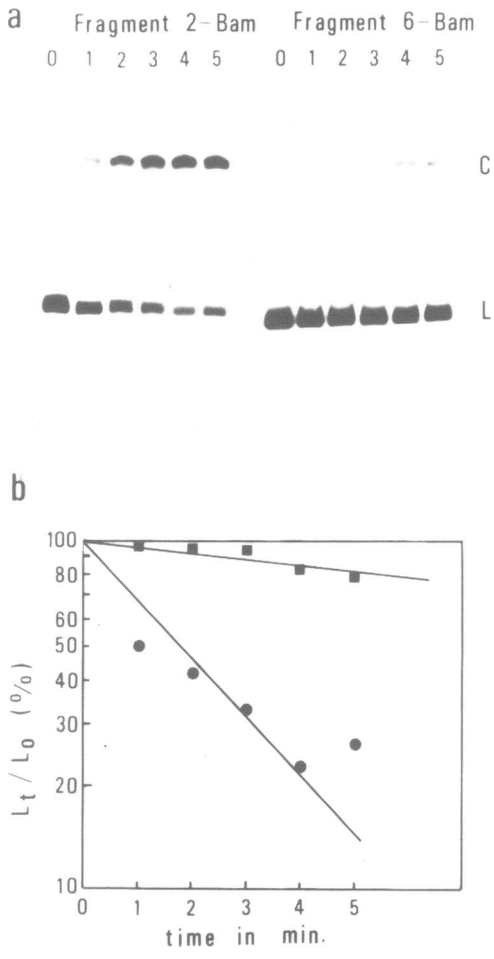

Fig. 3. DNA cyclization assay showing sequence-directed bend. (a) Kinetics of circularization. Numbers denote the time of ligation reaction (in minutes). C and L indicate the positions of the circle and the linear fragment, respectively. (b) The radioactivity of each linear band was measured by scanning the corresponding autoradiograms on a Shimadzu densitometer. ●, fragment 2-Bam; ■, fragment 6-Bam. L_t, linear fragments left at time t; L_0, linear fragments at time 0.

half). The second series of deletions, internal deletions, were denoted Δ X/Y, where X and Y indicate the 5' and 3' endpoints, respectively (Figure 4, lower half). Restriction fragments of these deletions were generated by cleaving with HinfI (upstream deletions) or with HinfI and Sau3A (internal deletions) so that the bend is close

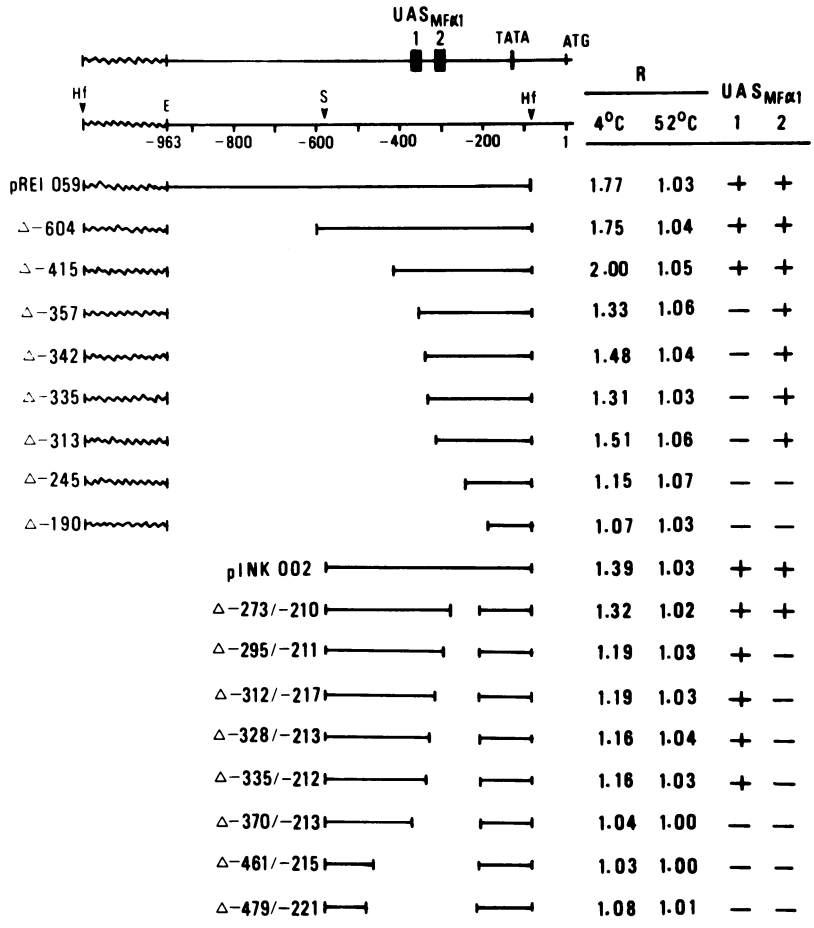

Fig. 4. Effect of deletions on DNA curvature. The deletion plasmids were digested with HinfI (upstream deletions, upper half) or with Sau3A and HinfI (internal deletions, lower half). The R value was measured as described in Materials and methods. Wavy line indicates DNA derived from the vector sequence. The column of $UAS_{MF\alpha1}$ represents the presence (+) or absence (-) of each $UAS_{MF\alpha1}$ element in individual deletions (9). Plasmids pREI059 and pINK002 have wild type DNA sequence. Expression levels are 6- to 11-fold less than that of wild type promoter for deletions lacking either one of the two $UAS_{MF\alpha1}$s. Deletions lacking both $UAS_{MF\alpha1}$s cannot express the MFα1 gene (9). S, Sau3A; Hf, HinfI; E, EcoRI.

to the center of the fragment. The results indicate that an anomalous slow electrophoretic mobility is closely related to the presence of each $UAS_{MF\alpha1}$ element on the DNA molecule. DNA fragments derived from

wild type (pREI059), Δ-604 and Δ-415, all of which carry both the $UAS_{MF\alpha1}$ elements, had dramatically anomalous electrophoretic behavior at 4°C ($R_{4°C} \geq 1.75$). DNA fragments from deletions lacking one of the $UAS_{MF\alpha1}$ elements, $UAS_{MF\alpha1}$-1, such as Δ-357, also migrated anomalously, but to a lesser extent than those containing both $UAS_{MF\alpha1}$s ($1.31 \leq R_{4°C} \leq 1.51$). In contrast, restriction fragments derived from deletions lacking both $UAS_{MF\alpha1}$s (Δ-245 and Δ-190) migrated with the appropriate electrophoretic mobility ($R_{4°C} \leq 1.15$). A similar result was obtained from internal deletions. R values at 4°C were over 1.3, between 1.16 and 1.19, and under 1.08 for DNA fragments containing both $UAS_{MF\alpha1}$s, only $UAS_{MF\alpha1}$-1 and neither of them, respectively. Mobilities of all these restriction fragments were close to normal when the gel was run at 52°C ($R_{52°C} \leq 1.07$).

Periodic repetition of runs of dA is thought to be responsible for sequence-directed bend and the net bend of a DNA molecule is thought to be resulted from the additive effects of small bends (27). Figure 5a shows nucleotide sequence around the $UAS_{MF\alpha1}$ region. This region contains two sets of (dA•dT) dinucleotides (tracts) phased nearly every 10.5 bp (-423 to -346 and -317 to -251), one overlaping $UAS_{MF\alpha1}$-1 and the other $UAS_{MF\alpha1}$-2. These periodical spaced (dA•dT) dinucleotides (tracts) seem to be important for the bent helical structure at the $UAS_{MF\alpha1}$ region. From these results we conclude that there exist two independent, sequence-directed bends.

Relative directions of the two bends

To elucidate the relative spatial orientation of two bends, we constructed a set of DNA fragments in which a spacer of various length was inserted between the two $UAS_{MF\alpha1}$ elements (Figure 5b). Electrophoretic behavior of the resultant fragments, differing only in the length of inserts, were analyzed on a polyacrylamide gel (Figure 6). When run at 4°C, mobilities of these fragments varied in a cyclical manner as the insertion length was varied from 0 to 44 bp (Figure 6a, c). The maximum of R values was observed for DNA fragments having inserts of 0, 20, 32 and 42 bp, nearly integral numbers of helical turn assuming 10.5 bp per turn. The R values of DNA fragments that harbour two bends should be maximum when the relative orientations of the bends are the same, that is, the end-to-end distance of the molecule is short, as indicated by Zinkel and

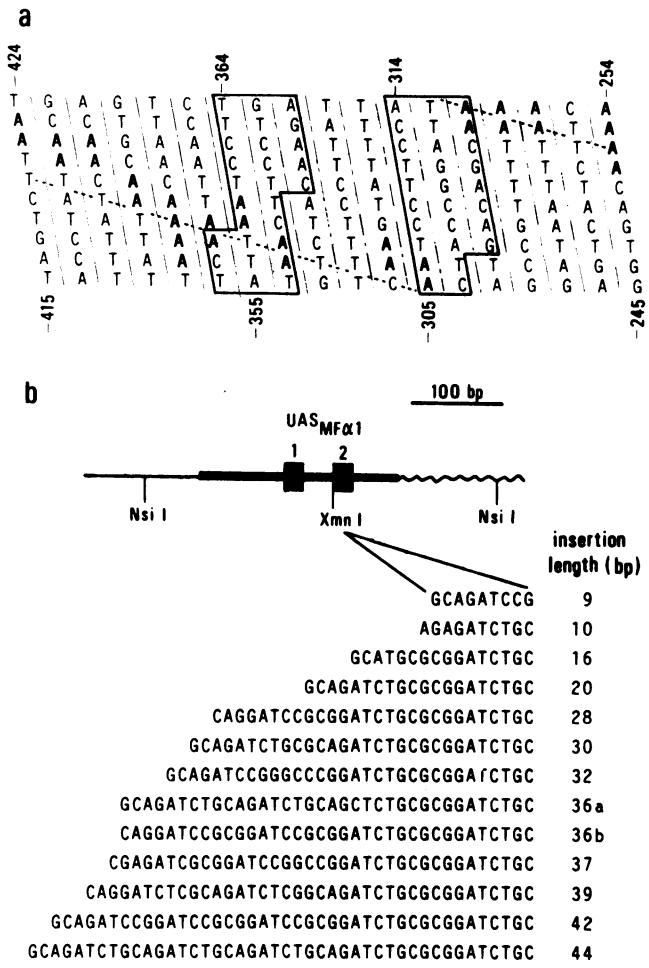

Fig. 5. Nucleotide sequences of the $UAS_{MF\alpha1}$ region (a) and insertion mutant series (b). (a) Sequence at the $UAS_{MF\alpha1}$ region is shown in a cylindical manner. dA runs regularly spaced with a periodicity of about 10 bp are indicated in bold type. Boxes indicate the two $UAS_{MF\alpha1}$ elements. The XmnI cleavage site used for construction of insertion mutants is between positions -314 and -313. Dotted line indicates the same face on the double helix assuming 10.5 bp per turn. The sequence is derived from reference 9. (b) Region around the $UAS_{MF\alpha1}$ elements of insertion series is shown schematically. Thick line, $UAS_{MF\alpha1}$ region; wavy line, TATA box region of CYC1; thin line, a region derived from URA3. Dark boxes represent the two $UAS_{MF\alpha1}$ elements. Nucleotide sequences of the insertion mutants were verified directly by DNA sequencing.

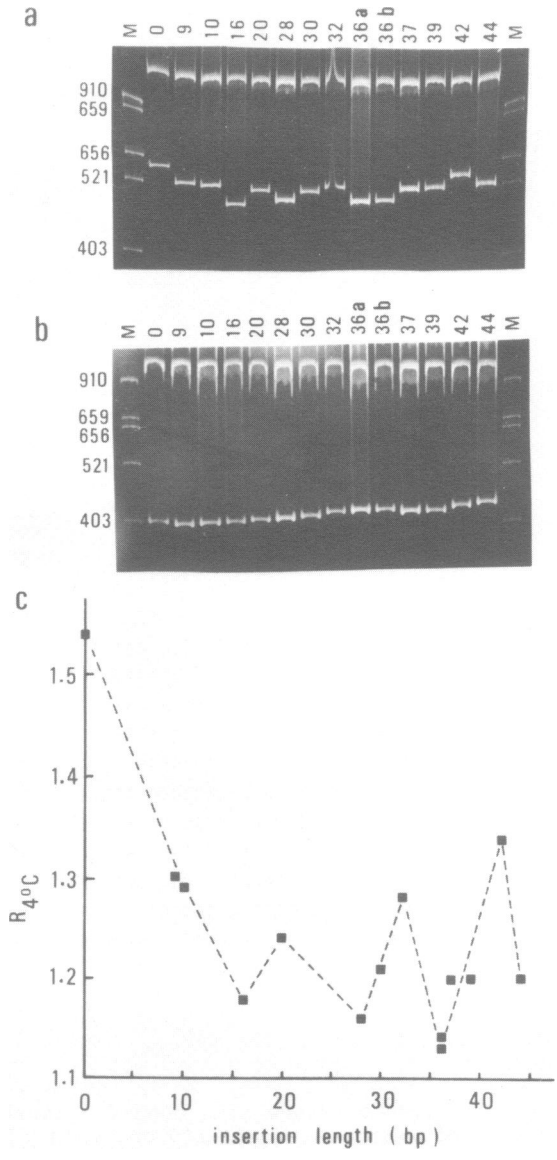

Fig. 6. Effect of insertions between two $UAS_{MFα1}$s on electrophoretic behavior of DNA fragments. Insertion mutant plasmids were digested with NsiI, ethanol-precipitated and applied onto a 7.5% polyacrylamide gel. Electrophoresis was done at 4°C (a) or at 52°C (b). The lanes are labeled with the length (bp) of inserted fragments. Lane M displays pBR322 DNA cut with AluI and the sizes (bp) are given on the left. Note that the 659 bp fragment shows retarded migration at 4°C. (c) R_{4^oC} is plotted against the insertion length (bp).

Crothers (33) and Salvo and Grindley (34). Mobilities at 52°C were close to normal (Figure 6b). Therefore, we conclude that the two bends on the wild type molecule lie in a nearly same plane with a same direction.

Bend at the regulatory region of STE3

DNA restriction fragments covering the regulatory region of STE3, another α-specific gene in S. cerevisiae, were examined for anomalous electrophoretic behavior. We found that DNA fragments containing the 117 bp region between the HhaI (-361) and FokI (-244) sites have shown an abnormally low mobility at 4°C ($R_{4^oC} \geq 1.24$)(Figure 7a). This region includes the UAS of the STE3 gene (35). The other restriction fragments had R_{4^oC} values below 1.12. All the fragments examined migrated almost normal when the gel was run at 52°C, indicating the presence of sequence-directed bend. Figure 7b shows nucleotide sequence around the UAS of STE3. The region includes several sets of (dA·dT) tracts phased nearly every 10.5 bp.

DISCUSSION

In this paper, we have provided several lines of evidence that a region responsible for transcriptional regulation of the MFα1 gene ($UAS_{MF\alpha1}$) contains sequence-directed bends of DNA helix axis. First, DNA molecules having the $UAS_{MF\alpha1}$ region migrated with an anomalously low mobility in polyacrylamide gel electrophoresis at low temperature. In contrast, mobility was close to normal when the gel was run at high temperature (Figure 1). This feature is a characteristic of the bent DNA molecule. Second, circular permutation analysis revealed that significant lower mobility is observed for DNA fragments having the $UAS_{MF\alpha1}$ elements near the center of the molecule. The mobility was almost normal when $UAS_{MF\alpha1}$ loci were close to the end of the fragment (Figure 2). This can be explained by the DNA bending model (14, 15); the bend center is located between the two $UAS_{MF\alpha1}$ elements. Finally, the rate of DNA cyclization for the circular permuatated molecule having $UAS_{MF\alpha1}$ at the center was significantly faster than that having these elements near the ends (Figure 3). Since the rate of cyclization would be dependent on the distance between the two ends, and since the end-to-end distance would be the shortest for a molecule having the bend at the center, this result confirms the sequence-directed bend at the $UAS_{MF\alpha1}$ region.

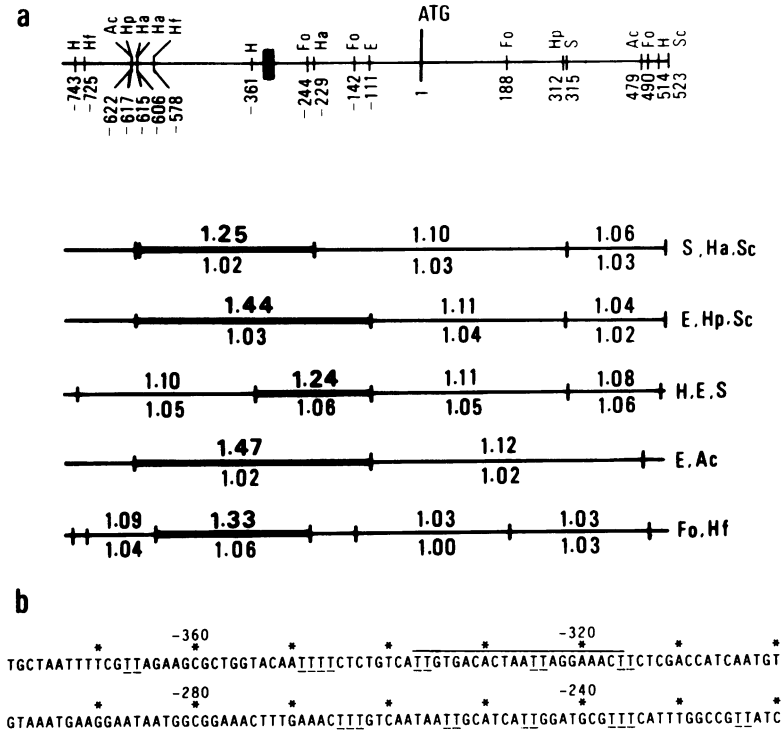

Fig. 7. Electrophoretic analysis of DNA fragments carrying the STE3 region. (a) DNA fragment carrying the STE3 gene derived from plasmid YCpSTE3HpK (37) was digested with the various restriction enzymes indicated, and the R value was measured as described in Materials and methods. The R value is indicated over (4°C) and under (52°C) the lines. Fragments where R>1.2 are indicated in bold type, and those where R_{4^oC} > 1.2 are indicated by thick lines. The dark box represents the UAS element (35). Sc, ScaI; Hp, HapII; Ac, AccI; Fo, FokI; Ha, HaeIII. Other abbreviations are as in Figure 1. (b) Sequence of the UAS region of STE3. dT runs regularly spaced with a periodicity of about 10 bp are underlined. Homologous sequence with $UAS_{MF\alpha1}$ is overlined. Nucleotides are numbered with respect to the first letter of the initiation codon (+1). The sequence is derived from reference 37.

Deletion analyses revealed the existence of two bends at the $UAS_{MF\alpha1}$ region, each of which overlaps each $UAS_{MF\alpha1}$ element (Figure 4). Almost all of the known bent regions contain periodically spaced runs of dA tracts with one run per helical repeat (see Introduction), and the net bend is thought to be resulted from the additive effects

of small bends associated with the dA runs (27). The nucleotide sequence at the $UAS_{MF\alpha1}$ region exhibits this feature; there exist two sets of dA runs repeating nearly every helical turn (9 to 12 nucleotides)(Figure 5a). Since each of the phased dA runs overlaps each $UAS_{MF\alpha1}$ element, these sequences seem to be determinants of the sequence-directed bends at the $UAS_{MF\alpha1}$ region. Both sets of the dA tracts face on the same side of the double helix assuming 10.5 bp per turn (Figure 5a), suggesting the relative orientations of the two bends to be nearly same. Insertion analysis indicates that this is the case (Figure 6). This is consistent with the result of a cyclization assay; if the two bends are in opposite orientation, the end-to-end distance of a molecule having the bends near the center would not differ significantly from that having them close to its ends.

We also show, in addition to UASs of the MFα1 gene, the existence of a sequence-directed bend at the UAS region of the STE3 gene (Figure 7). At present, we do not know whether the UAS region of the MFα2 gene, the other known α-specific gene (36), contains a sequence-directed bend, however, the bent helical structure seems to be a common feature at the regulatory region of α-specific genes and may play a role in transcriptional regulation of this set of genes. One possibility is that the bent helical structure is important for interaction between a regulatory protein(s) and an UAS element. UASs of α-specific genes are binding sites for the MATα1 protein, an α-cell-specific transcription activator, and for a protein(s), called PRTF, which is present in all three cell types, **a**, α and **a**/α (10; Inokuchi, unpublished data). Therefore, the MATα1 protein and PRTF may recognize a bent helical structure as well as a primary sequence of UAS elements. Importance of such a DNA structure for a protein recognition has been proposed for the origin region I of SV40 and the ompF promoter region (21, 26). Alternatively, the sequence-directed bends may modify the chromatin structure so that the proper regulation of gene expression can be achieved. Further studies will reveal a role of the bends in transcriptional regulation of this set of genes.

ACKNOWLEDGMENTS

We thank N. Nakayama for providing STE3 DNA, F. Ozawa for oligonucleotide synthesis, Y. Kikuchi for suggestions on the

manuscript and R. Matsuura for secretarial assistance. This work was supported by the Research and Development Project of Basic Technologies for Future Industries from the Ministry of International Trade and Industries of Japan.

*To whom correspondence should be addressed

REFERENCES

1. Guarente, L. (1984) Cell **36**, 799-800.
2. Struhl, K. (1987) Cell **49**, 295-297.
3. Guarante, L. and Hoar, E. (1984) Proc. Natl. Acad. Sci. USA **81**, 7860-7864.
4. Struhl, K. (1984) Proc. Natl. Acad. Sci. USA **81**, 7865-7869.
5. Kakidani, H. and Ptashne, M. (1988) Cell **52**, 161-167.
6. Webster, N., Jin, J. R., Green, S., Hollis, M. and Chambon, P. (1988) Cell **52**, 169-178.
7. Strathern, J., Hicks, J. and Herskowitz, I. (1981) J. Mol. Biol. **147**, 357-372.
8. Emr, S. D., Scheckman, R., Flessel, M. C. and Thorner, J. (1983) Proc. Natl. Acad. Sci. USA **80**, 7080-7084.
9. Inokuchi, K., Nakayama, A. and Hishinuma, F. (1987) Mol. Cell. Biol. **7**, 3185-3193.
10. Bender, A. and Sprague, G. F. (1987) Cell **50**, 681-691.
11. Sprague, G. F., Jensen, R. and Herskowitz, I. (1983) Cell **32**, 409-415.
12. Siliciano, P. G. and Tatchell, K. (1984) Cell **37**, 969-978.
13. Marini, J. C., Levene, S. D., Crothers, D. M. and Englund, P. T. (1982) Proc. Natl. Acad. Sci. USA **79**, 7664-7668.
14. Hagerman, P. J. (1984) Proc. Natl. Acad. Sci. USA **81**, 4632-4636.
15. Wu, H.-M. and Crothers, D. M. (1984) Nature **308**, 509-513.
16. Diekmann, S. and Wang, J. C. (1985) J. Mol. Biol. **186**, 1-11.
17. Griffith, J., Bleyman, M., Rauch, C. A., Kitchin, P. A. and Englund, P. T. (1986) Cell **46**, 717-724.
18. Burkhoff, A. M. and Tullius, T. D. (1987) Cell **48**, 935-943.
19. Zahn, K. and Blattner, F. R. (1985) Nature **317**, 451-453.
20. Zahn, K. and Blattner, F. R. (1987) Science **236**, 416-422.
21. Ryder, K., Silver, S., DeLucia, A. L., Fanning, E. and Tegtmeyer, P. (1986) Cell **44**, 719-725.
22. Deb, S., DeLucia, A. L., Koff, A., Tsui, S. and Tegtmeyer, P. (1986) Mol. Cell. Biol. **6**, 4578-4584.
23. Koepsel, R. R. and Khan, S. A. (1986) Science **233**, 1316-1318.
24. Snyder, M., Buchman, A. R. and Davis, R. W. (1986) Nature **324**, 87-89.
25. Bossi, L. and Smith, D. M. (1984) Cell **39**, 643-652.
26. Mizuno, T. (1987) Gene **54**, 57-64.
27. Koo, H.-S., Wu, H.-M. and Crothers, D. M. (1986) Nature **320**, 501-506.
28. Ito, H., Fukuda, Y., Murata, K. and Kimura, A. (1983) J.Bacteriol. **153**, 163-168.
29. Inokuchi, K., Furukawa, H., Nakamura, K. and Mizushima, S. (1984) J. Mol. Biol. **178**, 653-668.
30. Sanger, F., Nicklen, S. and Coulson, A. R. (1977) Proc. Natl.

Acad. Sci. USA **74**, 5463-5467.
31. Ulanovsky, L., Bodner, M., Trifonov, E. N. and Choder, M. (1986) Proc. Natl. Acad. Sci. USA **83**, 862-866.
32. Kotlarz, D., Fritsch, A. and Buch, H. (1986) EMBO J. **5**, 799-803.
33. Zinkel, S. S. and Crothers, D. M. (1987) Nature **328**, 178-181.
34. Salvo, J. J. and Grindley, N. D. F. (1987) Nucleic Acids Res. **15**, 9771-9779.
35. Jarvis, E. E., Hagen, D. C. and Sprague, G. F. (1988) Mol. Cell. Biol. **8**, 309-320.
36. Singh, A., Chen, E. Y., Lugovoy, J. M., Chang, C. N., Hitzeman, R. A. and Seeburg, P. H. (1983) Nucleic Acids Res. **11**, 4049-4063.
37. Nakayama, N., Miyajima, A. and Arai, K. (1985) EMBO J. **4**, 2643-2648.